DOI: 10.1002/chem.201100177

Crystal Structures and Repair Studies Reveal the Identity and the Base-Pairing Properties of the UV-Induced Spore Photoproduct DNA Lesion

Korbinian Heil,[a] Andrea Christa Kneuttinger,[a] Sabine Schneider,[b] Ulrike Lischke,[a] and Thomas Carell*[a]

In memory of Athel Beckwith

Abstract: UV light is one of the major causes of DNA damage. In spore DNA, due to an unusual packing of the genetic material, a special spore photoproduct lesion (SP lesion) is formed, which is repaired by the enzyme spore photoproduct lyase (Spl), a radical *S*-adenosylmethionine (SAM) enzyme. We report here the synthesis and DNA incorporation of a DNA SP lesion analogue lacking the phosphodiester backbone. The oligonucleotides were used for repair studies and they were cocrystallized with a polymerase enzyme as a template to clarify the configuration of the SP lesion and to provide information about the base-pairing properties of the lesion. The structural analysis together with repair studies allowed us to clarify the identity of the preferentially repaired lesion diastereoisomer.

Keywords: DNA damage · enzymes · oligonucleotides · spore photoproduct · UV irradiation

Introduction

Genetic material is strongly protected in bacterial spores, which were designed by nature to store DNA material over long periods of time.[1] Spores can protect the genetic information for over thousands of years, which make them the most sophisticated and durable information storage systems on earth. DNA packed inside a spore is also more resistant towards UV light, which is otherwise an agent that constantly damages DNA on earth in light-exposed habitats.[2] Despite this unusual UV-light resistance, it is known that spore DNA is also at some point damaged by UV light. In contrast to normal DNA, however, where UV light causes the formation of cyclobutane pyrimidine dimers (CPDs) and pyrimidine(6–4)pyrimidones ((6–4) lesions), in spores an unusual lesion accumulates, which is called the spore photoproduct lesion.[3] This lesion hinders the ability of spores to restore gene function upon germination. The spore lesions are repaired by special, oxygen-sensitive, radical *S*-adenosylmethionine (SAM) enzymes, which are able to locate the lesions and to perform a direct repair.[4] These spore photoproduct lyases (Spl) form, next to CPD photolyases and (6–4) photolyases, a third enzyme family, which is able to directly repair mutagenic UV lesions. Repair by the Spl is a radical process, which is initiated by a protein-bound iron–sulfur cluster and which requires the cofactor SAM.[5] The mechanism that leads to the formation of the spore lesion is still not completely understood. It is believed that triplet states are involved and it is clear that the photosensitizer dipicolinic acid and dry conditions favor formation of the lesion.[6] So far, formation of the lesion was only observed in thymidylyl–(3′–5′)–thymidine (TpT) sequences, in which, by an unknown process, one of the methyl groups present at one thymine reacts at the C5 position of the second thymine base (Scheme 1).[7] This reaction creates a new stereocenter

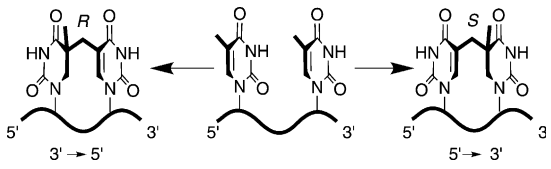

Scheme 1. Depiction of the two possible spore photoproducts with 5*S* and 5*R* configuration.

at C5. In addition, the new bond can form between the C5 carbon atom of the 5′dT base and the 3′dT-methyl group (5′→3′) or vice versa. This leads in principle to four different spore lesions. Due to the geometrical constraints imposed by the B-duplex structure, reaction in the 5′→3′ direction, however, must give the 5*R*-configured lesion, whereas reaction in the 3′→5′ direction should provide the 5*S*-configured compound (Scheme 1) making these two diastereoisomers

[a] Dipl.-Chem. K. Heil, A. C. Kneuttinger, Dipl.-Biol. U. Lischke, Prof. Dr. T. Carell
Center for Integrated Protein Science (CiPS^{M}) at the Department of Chemistry, Ludwig-Maximilians-University
Butenandtstrasse 5–13, 81377 Munich (Germany)
E-mail: thomas.carell@cup.uni-muenchen.de

[b] Dr. S. Schneider
Department of Chemistry
Technical University of Munich
Lichtenbergstrasse 4, 85747 Garching, Munich (Germany)

Supporting information for this article is available on the WWW under http://dx.doi.org/10.1002/chem.201100177.

the only possible spore photoproduct (SP) lesions formed in the duplex.

Recently, we reported the synthesis of 3′→5′ lesion analogues with 5*S* and 5*R* configurations as phosphoramidite building blocks and showed the preparation of DNA duplexes containing both compounds.[8] The 5*S* isomer was indeed found to create the more stable duplex proving that the 3′→5′ reaction would form preferentially the 5*S*-configured lesion. Initial studies with a dinucleotide building block provided evidence that the Spl is able to repair the 5*S* compound.[9] Recent seminal studies by the groups of Broderick and Bardet showed, however, that the SP lesion forms exclusively in the 3′→5′ direction with the 5*R* configuration and that the 5*R* compound is the preferred substrate for the repair enzyme.[10] We report here the development of a synthesis of the 5*S*- and 5*R*-configured 5′→3′ reaction products as phosphoramidite building blocks, their incorporation into oligonucleotides, and repair studies, now with full oligonucleotides. Our prepared lesions are again analogues that lack the central phosphodiester group to abbreviate the long and challenging synthesis of the natural spore lesion, as well as to ease the analysis of the repair reaction, which gives with our analogues an easy-to-detect strand break. Finally, we report crystal structures of DNA duplexes containing the 5*S* and 5*R* 5′→3′ reaction products using a DNA polymerase as a crystallization template. The structure provides insight into the base-pairing properties of both compounds, most importantly for the biologically relevant 5*R*-configured 5′→3′ molecule.

Results and Discussion

The synthesis of the two phosphoramidites is depicted in Scheme 2. The starting point of the synthesis is thymidine **1**, which was firstly TBDPS-protected at the primary OH group, secondly TBS-protected at the secondary OH groups, thirdly SEM-protected at the ring nitrogen, and finally brominated to give the fully protected allyl bromide **2**. The second building block was prepared from compound **1** by firstly hydrogenation, secondly TBS protection, and TBDPS protection of the primary and secondary OH groups, respectively, followed by final SEM protection of the ring nitrogen to give compound **3** (Scheme 2). Enolate–allyl bromide coupling furnished the coupled dinucleotide **4** as a diasterotopic mixture.[11] Separation of the two diastereoisomers was possible after TBS-group cleavage to give compound **5** and **6** after isocratic normal-phase HPLC on a silica-gel column with ethyl acetate (38%), *n*-heptane (58%), and a small percentage of isopropanol (4%). The isopropanol helps to separate residual compound **3** from the reaction mixture. Compounds **5** and **6** were subsequently protected by using DMT and the secondary OH groups were converted to the corresponding phosphoramidites **7** and **8**. Incorporation of both compounds into DNA was performed using standard phosphoramidite DNA synthesis with slightly modified conditions, in which only the coupling times were doubled. To

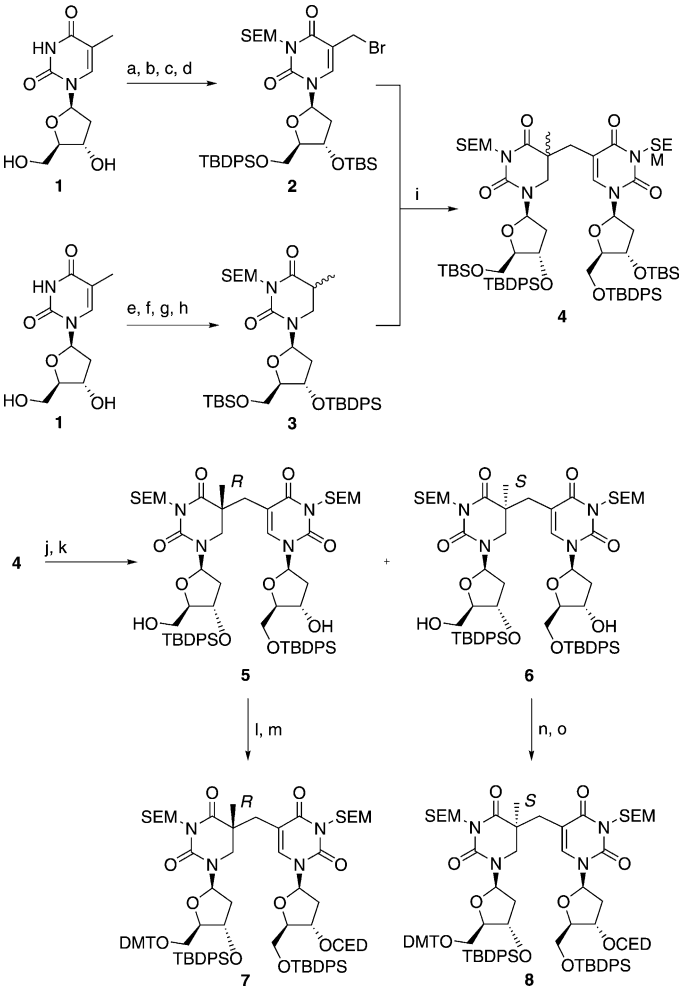

Scheme 2. Synthesis of the phosphoramidite building blocks **7** and **8**. a) *tert*-Butylchlorodiphenylsilane (TBDPSCl), 4-dimethylaminopyridine (DMAP), 75%; b) *tert*-butyldimethylsilyl chloride (TBSCl), imidazole, 99%; c) 2-(trimethylsilyl)ethoxymethyl chloride (SEMCl), *N*,*N*-diisopropylethylamine (DIEA), 61%; d) *N*-bromosuccinimide (NBS), azobisisobutyronitrile (AIBN), 50%; e) H_2, Rh/Al_2O_3, 98%; f) TBSCl, DMAP, 79%; g) TBDPSCl, imidazole, 99%; h) SEMCl, DIEA, 80%; i) lithium diisopropylamide (LDA) then **2**, −78°C to RT; j) toluene sulfonic acid (*p*TsOH), 50°C; k) normal-phase (np) HPLC separation of diastereoisomers (ds) **5** (8%) and **6** (5%) over 3 steps; l) 4,4′-dimethoxytriphenylmethyl chloride (DMTCl), DMAP, 66%; m) 2-cyanoethyl *N*,*N*-diisopropylchlorophosphoramidite (CEDCl), DIEA, 66%; n) DMTCl, DMAP, 64%; o) CEDCl, DIEA, 44%.

remove the SEM groups after DNA synthesis, the solid-phase material containing the oligonucleotides was treated with $SnCl_4$ in CH_2Cl_2 for 1 h at room temperature. This is a critical step because of the general sensitivity of nucleic acids towards acids and also Lewis acids. After removal of the deprotection solution, the SEM-deprotected oligonucleotides were cleaved from the resin with concomitant cleavage of the standard nucleobase protecting groups with NH_3 in ethanol/water. The crude oligonucleotides were subsequently treated with **3**·HF-Et_3N to remove the TBDPS groups. The DNA was finally purified by reversed-phase HPLC using a water/acetonitrile gradient with an

Et_3N·HOAc buffer. The integrity of the oligonucleotides was investigated with MALDI-TOF mass spectrometry. The sequences of the prepared oligonucleotides together with the calculated and found molecular weights are depicted in Table 1.

Table 1. Depiction of the prepared oligonucleotides ODN1 and ODN2 using compounds **7** and **8**. ODN3 and ODN4 are the counter strands used for crystallization and repair assays, respectively. ODN5 and ODN6 are the expected product strands of the repair reaction.

Number	Sequence (5′→3′)	$[M-H]^-$ (calcd)	$[M-H]^-$ (found)
ODN 1	AGGGT(*R*-SP)TGGTC	3036	3035
ODN 2	AGGGT(*S*-SP)TGGTC	3036	3036
ODN 3	ATGCGACCAACCCT	4194	4195
ODN 4	GACCAACCCT	2957	2957
ODN 5	TGGTC	1495	1496
ODN 6	AGGGT	1544	1544

To unequivocally assign the stereochemistry at the C5 position of the spore lesion analogues and to investigate the pairing properties of both lesions in the duplex, we used the possibility to crystallize DNA in the complex with the DNA polymerase from *Geobacillusstearothermophilus* (*Bacillus stearothermophilus*, *B. st.* Pol I).[12] For this study we placed the lesion not in the active site of the polymerase but in the double-stranded region to study the lesion in a B-duplex environment. Indeed, upon combining a solution of the spore lesion analogue-containing DNA duplexes ODN1:ODN3 and ODN2:ODN3 (with the lesion positioned 5 bases away from the active site) and a solution of the *B. st.* Pol I protein gave, under suitable conditions (45–50 % $(NH_4)_2SO_4$, 3.5–4.5 % 2-methyl-2,4-pentanediol (MPD), and 100 mM 2-(*N*-morpholino)ethanesulfonic acid (MES), pH 5.8, hanging-drop vapor diffusion method), crystals that diffracted X-rays to a resolution of 2.15 (5*R*) and 2.80 Å (5*S*). The absolute stereoconfiguration, determined with this crystallographic method is in agreement with the recent papers from Bardet and Broderick,[10b,c] thereby showing that older assignments led to erroneous conclusions.[11]

Figure 1a shows a schematic representation of the structure. Figure 1b provides a magnification of the lesion, together with an example of the electron density. The result of the structure with the 5*R* lesion is that this diastereoisomer fits quite well into the DNA duplex and that it forms two almost perfect Watson–Crick base pairs with the two opposite adenines with hydrogen-bond lengths between 3.1 and 2.9 Å (see Figure S1 in the Supporting Information). It is also notable that the missing phosphodiester backbone does not seem to disturb the structure. Overlay of our structure with a structure of *B. st* Pol I in complex with undamaged DNA (pdb entry 1NJY) shows that the phosphate of the undamaged oligonucleotide fits perfectly between the 3′ OH group of the thymidine and the 5′ hydroxyl group of the 5,6-dihydrothymidine part of the lesion (Figure 1c).[13] The two heterocycles of the 5*R* spore lesion are at an angle of approximately 30° to form the new bond and the glycosidic

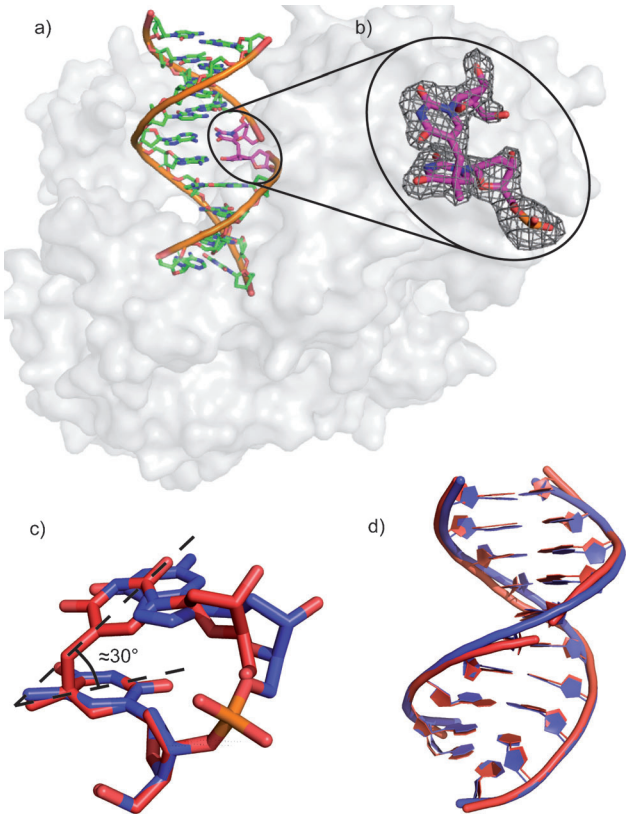

Figure 1. Depiction of the crystal structure of the 5′→3′ 5*R* spore photoproduct analogue-containing duplex in complex with *B. st.* Pol I (pdb entry 2y1j). a) *B. st.* Pol I in complex with the 5*R*-lesion-containing DNA. b) Enhanced representation of the 5*R* spore photoproduct with overlaid electron density. c) Overlay of the lesion (red) and of an undamaged DNA segment (blue). d) Overlay of undamaged DNA and the spore photoproduct-containing DNA bound to the enzyme.

bonds are at an angle of 20°. The glycosidic bonds in a dipyrimidine sequence are almost parallel (≈5° for 1NJY), making the angle between the glycosidic bonds a good indicator of backbone distorsion. Interesting is a comparison with the structures of the other UV-induced lesions shown in Figure 2. Cyclobutane pyrimidine dimer (CPD) lesions, such as the T(CPD)T lesion (Figure 2b), are considered to disturb the duplex structure only slightly. Here, however, the two 5,6-dihydrothymine rings are arranged at an angle of about 50° and the glycosidic bonds at about 30° (pdb entry 3MR3, see Figures S2 and S3 in the Supporting Information).[14] For the other two major UV-induced lesions, the (6–4) lesions (Figure 2c, pdb: 3CVU) and the Dewar lesions (Figure 2d, pdb: 2WQ6), the structural changes are much more dramatic (see Figure 2).[15] In comparison to all these UV-induced lesion structures, the result of our study is that formation of the 5′→3′ 5*R* spore lesion induces by far the smallest changes. This result is supported by a complete overlay of the 5*R* lesion-containing DNA with undamaged DNA (Figure 2d). The overall structural perturbation caused by the 5′→3′ 5*R* lesion is only minimal.

The argument that the structural perturbations are small because the duplex is stiffly held by the enzyme in the B

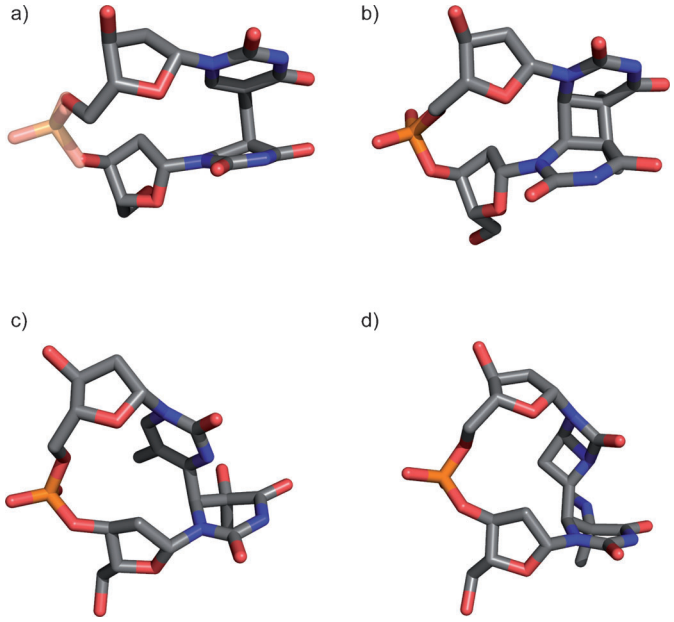

Figure 2. Crystal structures of the four major photo lesions: a) spore photoproduct (pdb entry 2yli), b) T(CPD)T (3MR3),[14] c) T(6–4)T (3CVU),[15b] and d) T(Dew)C* (2WQ6).[15a] Note that the phosphodiester present in the SP lesion structure (a) was inserted by modeling (shown with 50% transparency).

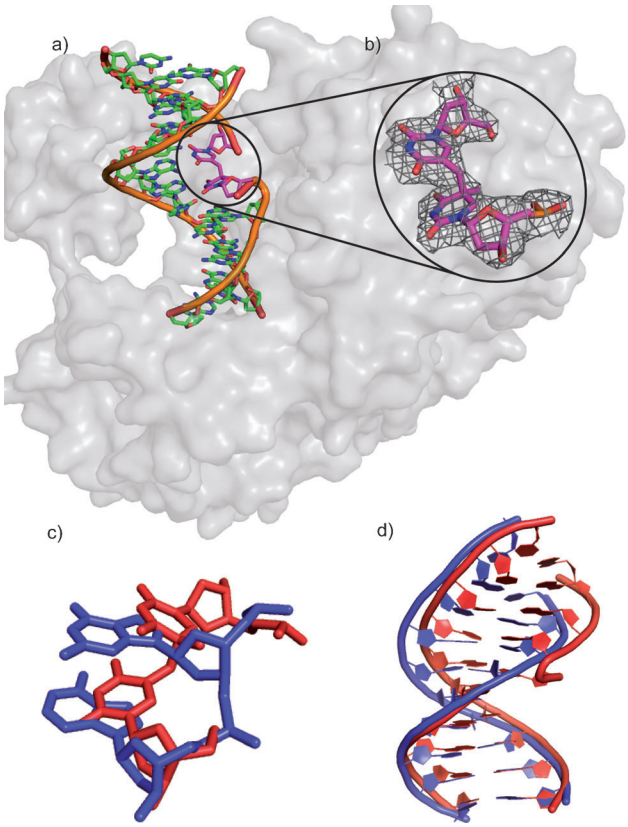

Figure 3. Depiction of the crystal structure of the 5*S* spore photoproduct analogue-containing duplex in complex with *B. st.* Pol I (pdb entry 2y1i). a) Molecular architecture of *B. st.* Pol I in complex with the 5*S* lesion-containing DNA. The enzyme is represented as surface (gray). The DNA (green) is shown as a stick model with the lesion highlighted in pink. The phosphate backbone is shown as a sketch. b) Enhanced representation of the 5*S* spore photoproduct with overlaid electron density. c) Alignment of the complex with undamaged DNA bound to *B. st.* Pol I (1NJY). The 3′ thymidine together with its sugar is completely turned. d) Overall overlay of the undamaged DNA (1NJY) and the spore photoproduct-containing DNA. Normal Watson–Crick base paring is impossible for the lesion.

structure was investigated with the duplex containing the 5′→3′ 5*S* lesion. The structure of the *B. st.* Pol I in complex with the duplex containing the 5*S* lesion analogue is provided in Figure 3a. A magnification of the lesion and a part of the electron density is shown in Figure 3b. The overlay with a complex of undamaged oligonucleotides bound to *B. st.* Pol I is presented in Figures 3c and d (pdb: 1NJY). In this structure we detect that the 5,6-dihydrothymidine is fully turned around the bond between the C5-methyl group and the C5 atom even if bound to the enzyme, thereby proving that the structural analysis is able to report duplex perturbations. We were unable to model a hypothetical phosphodiester group between the two free hydroxyl groups of the sliced backbone due to the tremendous distortion, which shows that this 5*S* analogue is unable to fit into the duplex. It is a hypothetical possible diastereoisomer of the spore lesion, which cannot form due to the duplex environment in which the lesion formation process has to take place. However one should keep in mind that the DNA is bound to a protein and that the duplex distortion may change in solution.

To investigate whether the oligonucleotide containing the 5*R*-configured 5′→3′ lesion is accepted as a substrate as expected by the Spl enzyme we treated the two single strands ODN 1 and ODN 2 individually with the SplG enzyme from *Geobacillusstearothermophilus* at 37 °C and analyzed the reaction mixture by HPLC.[16] The lack of a phosphodiester backbone enabled us to detect the repair reaction through the simple analysis of a strand break that occurs only when repair takes place. The two thymidines are no longer connected after repair. Two shorter DNA product strands are formed (ODN 5 and ODN 6, see Table 1). Figure 4a shows the results obtained for the 5*R* isomer. Line (I) depicts the situation of the repair assay after addition of the enzyme and SAM under anaerobic conditions. The starting material ODN 1 disappeared and two new peaks are visible. To prove that these new peaks are formed by ODN 5 and ODN 6, we prepared a mixture of synthetic ODN 1, ODN 5, and ODN 6 and analyzed the mixture of these three oligonucleotides under the same HPLC conditions. The data, shown in line (II), are identical to those obtained from the original enzyme assay. Finally a co-injection experiment with the assay solution taken after complete repair was performed (line (III)) showing again that the newly formed peaks are caused by ODN 5 and ODN 6. ODN 1 containing the 5*R*-configured 5′→3′ lesion product is as a result efficiently repaired.

Figure 4b shows the results obtained with ODN 2, which contained the incorporated 5′→ 3′ 5*S* lesion analogue. The HPLC chromatogram of assay (I) shows only the starting

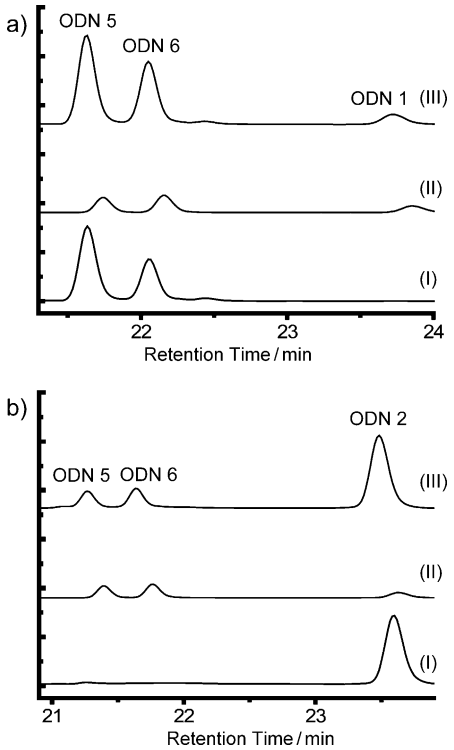

Figure 4. Depiction of the HPLC analysis of the repair assay at 37 °C. The spore photoproduct-containing DNA was incubated together with the spore photoproduct lyase. a) Depiction of the results obtained with the 5*R* analogue-containing ODN 1. (I) shows the reaction mixture. Here, only the oligonucleotides ODN 5 and ODN 6 are visible and the lesion is consequently fully repaired. Line (II) shows a mixture of synthesized ODN 1, ODN 5, and ODN 6. Line (III) shows the co-injection of the mixture (II) to the assay solution. No new peaks, aside from ODN 1, appear, proving that the peaks in (I) are the repaired strands ODN 5 and ODN 6. b) Depiction of the repair results obtained with ODN 2 containing the 5*S* analogue. In (I) only the starting material (ODN 2) is visible. No repair occurs. Line (II) shows a mixture of synthesized ODN 2, ODN 5, and ODN 6. Line (III) shows the co-injection of the mixture (II) to the assay solution. No new peaks, aside from ODN 5 and ODN 6 appear.

material ODN 2. The chromatograms of the mixture of synthesized ODN 5, ODN 6, and ODN 2 shown in (II) and the co-injection of this mixture and the assay solution, provided in (III), prove that the 5*S* lesion is not repaired.

Since DNA is naturally double stranded, the assays were repeated with the lesion-containing duplexes ODN1:ODN4 and ODN2:ODN4. The temperature was reduced to 20 °C to avoid melting of the duplex during the repair reaction and increased to 60 °C during the HPLC analysis to ensure single-stranded oligonucleotides for the analysis (see Figure S4 in the Supporting Information). Again, repair was observed for the 5′→3′ 5*R* lesion, whereas the 5′→3′ 5*S* lesion showed no reaction. Due to the unsuitable temperature for a thermophilic enzyme and the lower kinetics, caused by the duplex, the reaction proceeded with only about 70% yield.

Conclusion

We present the synthesis of both diastereoisomers (5*R* and 5*S*) of the 5′→3′ spore photoproduct as phosphoramidites with an open backbone. These phosphoramidites enabled the incorporation of the lesion analogues into oligonucleotides by using standard solid-phase synthesis in combination with an elaborate multistep oligonucleotide-deprotection protocol. Together with previous synthetic results from our laboratory, which show incorporation of the backbone-opened 3′→5′ 5*S* and 5*R* lesion analogues, the whole set of the 4 possible spore lesions can now be prepared and inserted into DNA.[8] Repair studies show that the 5′→3′ 5*R* analogue, incorporated in oligonucleotides, is efficiently repaired. Crystallization of a DNA duplex containing the 5′→3′ 5*R* compound in complex with a polymerase, which was used only as a crystallization matrix, with the compound situated in a duplex-binding region of the protein, shows that the lesion disturbs the duplex only slightly, in comparison with double-stranded DNA bound to the same protein. In fact, in comparison with structures of the other main UV-induced lesions, (CPD, (6–4), and Dewar) the 5′→3′ 5*R* spore lesion induces only minor structural perturbations. In the lesion, both thymines form almost perfect Watson–Crick hydrogen bonds to the opposite adenine base-pairing partners. The structure obtained here allows modeling of a phosphodiester group between the two 3′ and 5′ OH groups present on the sugar molecules, which shows that the lack of these groups affect the overall structure only slightly. In the lesion the two thymine heterocycles are stiffly connected by means of a covalent bridge and embedded in the B-duplex environment. The 5′→3′ 5*S* lesion analogue in contrast disturbs the duplex significantly and more importantly it is impossible to model a phosphodiester bridge between the two 2-deoxyribose units, thereby showing that this hypothetical compound does not fit into the duplex, in full agreement with the idea that the structural constraints of the B-duplex prohibit formation of the 5*S* spore photoproduct. Together with our previous study of the two 5*S*/*R* 3′→5′ compounds, we can conclude that indeed only the two spore lesions 5*S* 3′→5′ and 5*R* 5′→3′ can form in the duplex. In the 5′→3′ case it is the 5*R* compound that is efficiently repaired. For the analysis of the spore lesion formation and repair processes it is important to analyze critically which reaction products 5′→3′ versus 3′→5′ one analyzes. This has also affected a previous repair analysis by us, in which the different reaction directions were not sufficiently considered.[9b,23]

Experimental Section

General: The *Escherichia coli* strain Tuner(DE3)pLysS (Novagen) and the pDEST17 expression vector (Invitrogen) were used for overexpression of SplG. The BugBuster 10X protein-extraction reagent was purchased from Novagen and the nickel–nitrilotriacetic acid (Ni–NTA) superflow resin was from Qiagen. *S*-Adenosylmethionine was obtained from Sigma–Aldrich and used without further purification. Other chemicals and solvents were purchased from ABCR, Alfa Aesar, Acros, Fluka,

Sigma–Aldrich, or TCI in the qualities puriss., p.a., or purum. Dry solvents (<50 ppm H_2O) were obtained from Fluka and Acros. All reactions employing dry solvents were performed under an inert atmosphere (N_2). Technical-grade solvents were distilled prior to use for column chromatography and liquid–liquid extractions on a rotary evaporator (HeidolphLaborota 4000). Reaction products were dried under high vacuum (10 mbar). Aqueous solutions were dried on a SpeedVac plus CS110A or SPD 111V from Savant or lyophilized (Christ ALPHA 2-4). Thin-layer chromatography (TLC) was performed with aluminum plates (silica gel 60 F254, 10×5 cm). Substances were visualized by illumination with UV light ($\lambda = 254$ nm). ESI-MS was performed on a Finnigan LTQ Fourier transform ion cyclotron resonance (FTICR) spectrometer. MALDI-TOF was performed on a BrukerAutoflex II. NMR spectra were recorded on the following spectrometers: Varian Oxford 200, Bruker AC 300, Varian XL 400, and Bruker AMX 600.

Oligonucleotide synthesis and deprotection: The experiments were performed on an Expedite 8909 nucleic acid synthesis system (PerSeptive-Biosystems) using standard DNA synthesis conditions. Phosphoramidites for dA, dC, dG, dT, and CPG carriers were obtained from Amersham, Glen Research, or PE Biosystems. SEM-protecting groups were removed by rinsing the 0.2 mmol cartridges with 1 M $SnCl_4$ in CH_2Cl_2 (20 mL) over 1 h at room temperature under dry conditions, followed by rinsing with CH_2Cl_2 (20 mL). The oligonucleotides were removed from the resin with concomitant cleavage of the standard nucleobase protecting groups by treatment with concentrated NH_3 in water/ethanol 3:1 (1 mL) at room temperature for 18 h. The solution was decanted from the resin and dried in a speed vacuum. For cleavage of the TBDPS groups the residue was heated at 65 °C in a mixture of anhydrous DMSO (100 μL) and triethylamine trihydrofluoride (TEA·3 HF) (125 μL) for 1 h. After precipitation in butanol and HPLC purification the oligonucleotides containing the lesion analogues were obtained in yields of about 15%, with respect to the resin loading.

HPLC: Separation of the diastereoisomers was performed on a Merck-Hitachi system (L-7400 UV detector, L-7480 fluorescence detector, L-7100 pump) using a VP 250/40 Nucleodur 100-5 column from Macherey–Nagel (isocratic ethyl acetate/heptanes/isopropanol). Purification and analysis of the ODNs was performed on a Waters system (Alliance 2695 with PDA 2996; preparative HPLC: 1525EF with 2484 UV detector) with VP 250/10 Nucleodur 100-5 C18 ec and VP 250/4 Nucleodur 100-5 C18 ec columns from Macherey–Nagel using a gradient of 0.1 M triethylamine/acetic acid in water and 80% acetonitrile.

HPLC-ESI-MS: The samples (100 μL injection volume) were analyzed by HPLC-ESI-MS on a Thermo Finnigan LTQ Orbitrap XL and were subjected to chromatography with a Dionex Ultimate 3000 HPLC system using a gradient of 2 mM ammonium formate in water and 80% acetonitrile over an Uptisphere120-3HDO column from Interchim.

***B. st.* Pol I purification, crystallization, and structure determination**: *B. st.* Pol I was overproduced, purified, and cocrystallized with the lesion-containing duplexes by using published procedures.[12] Data were collected at the PX III (Swiss Light Source (SLS), Villigen, Switzerland) and processed with the programs XDS[17] and SCALA.[18] Structure solution was carried out by molecular replacement with PHASER[19] using the coordinates of PDB code 1U45. To reduce model bias, prior to model building in COOT[20] the temperature factors were reset to the Wilson B factor and a simulated annealing omit map, with the area around the lesion removed, was calculated with PHENIX.[21] Restrained refinement was carried out in REFMAC5.[22] All structural super positions and structural figures were prepared with Pymol (Delano Scientific). Data processing and refinement statistics are summarized in Table S5 in the Supporting Information.

Expression and purification of recombinant SP lyase: The gene coding for the SplG (UniProt accession ADU94823) from *Geobacillusstearothermophilus* DSM No. 22 was amplified using the polymerase chain reaction (PCR) from genomic DNA using the primers 5′-CACCATGAAACCGTTTGTGCCAAAACTT-3′ and 5′-TTACGTAAAATACTGCACTTGGG-3′ (Metabion). The PCR product was cloned using the Gateway system (Invitrogen) first into the entry vector pENTR/TEV/D-TOPO and further transferred into the destination vector pDEST17 coding for an N-terminal His_6 tag. For protein expression, transformed Tuner(DE3)pLysS (Novagen) cells were grown in Luria Bertani medium supplemented with carbenicillin (100 μg mL^{-1}) and Fe^{III}–citrate (100 μM) at 37 °C. Protein expression was induced with 1 mM isopropyl β-D-thiogalactopyranoside (IPTG) at 22 °C ($OD_{600} = 0.6$–0.7). After 1 h at 22 °C, the culture was cooled to 4 °C and incubated overnight for 13–15 h. Cells were harvested by centrifugation and transferred into a glovebox and all following steps were performed under anaerobic conditions. Cell lysis was carried out using 10× BugBuster (Novagen) in 50 mM HEPES, 300 mM NaCl, 0.5% Tween-20, and 5 mM β-mercaptoethanol, pH 8.0. The protein was purified by nickel-affinity chromatography in a batch method. The column was washed with 50 mM HEPES, 300 mM NaCl, 15 mM imidazole, 0.5% Tween-20, and 5 mM β-mercaptoethanol, pH 8.0, and the protein was eluted with 50 mM HEPES, 300 mM NaCl, 200 mM imidazole, and 5 mM β-mercaptoethanol, pH 8.0. The protein sample was concentrated in 50 mM HEPES (pH 8.0), 300 mM NaCl, and 5 mM dithiothreitol (DTT) by centrifugal filter devices and stored at 4 °C and used for the repair assays within one day without further purification.

Assay for DNA repair: To ensure full reduction, prior to the DNA repair assay, the enzyme was incubated for at least 1 h with 4 mM Na dithionite. To investigate DNA repair, 6 nmol of SplG were incubated with 2 nmol single-stranded lesion-containing DNA. The reaction mixture further contained 3 mM Na dithionite, 5 mM dithiothreitol (DTT), and 1 mM SAM. After 14–16 h at 37 or 20 °C, respectively, the protein was removed by precipitation and centrifugation and the supernatant was stored at −20 °C until HPLC analysis.

Accession numbers: Atomic coordinates and structure factors (PDB entries 2yli; 2ylj) of the protein in complex with DNA have been deposited in the PDB at the EBI Macromolecular Structure Database (http://www.ebi.ac.uk/pdbe).

Acknowledgements

We thank the Excellence Cluster CiPS^M and SFB 749 for financial support and the beamline staff at the SLS for setting up the beamlines and for helpful advice.

[1] C. Desnous, D. Guillaume, P. Clivio, *Chem. Rev.* **2010**, *110*, 1213–1232.
[2] a) T. Carell, *Angew. Chem.* **1995**, *107*, 2697–2700; *Angew. Chem. Int. Ed. Engl.* **1995**, *34*, 2491–2494; b) A. Sancar, *Chem. Rev.* **2003**, *103*, 2203–2237; c) J. Cadet, E. Sage, T. Douki, *Mutat. Res. Fund. Mol. Mech. Mutagen.* **2005**, *571*, 3–17; d) J.-S. Taylor in *DNA Damage Recognition* (Eds.: W. Siede, Y. Wah Kow, P. W. Doetsch), CRC Press, **2005**; e) K. Heil, D. Pearson, T. Carell, *Chem. Soc. Rev.*, DOI: DOI: 10.1039/C000407N.
[3] J. E. Donnellan, Jr., R. B. Setlow, *Science* **1965**, *149*, 308–310.
[4] a) N. Munakata, C. S. Rupert, *J. Bacteriol.* **1972**, *111*, 192–198; b) P. Fajardo-Cavazos, C. Salazar, W. L. Nicholson, *J. Bacteriol.* **1993**, *175*, 1735–1744; c) P. Setlow, *Annu. Rev. Microbiol.* **1995**, *49*, 29–54; d) R. Rebeil, W. L. Nicholson, *Proc. Natl. Acad. Sci. USA* **2001**, *98*, 9038–9043; e) T. A. Slieman, R. Rebeil, W. L. Nicholson, *J. Bacteriol.* **2000**, *182*, 6412–6417; f) J. M. Buis, J. Cheek, E. Kalliri, J. B. Broderick, *J. Biol. Chem.* **2006**, *281*, 25994–26003.
[5] a) A. Chandor-Proust, O. Berteau, T. Douki, D. Gasparutto, S. Ollagnier-de-Choudens, M. Fontecave, M. Atta, *J. Biol. Chem.* **2008**, *283*, 36361–36368; b) J. Cheek, J. B. Broderick, *J. Am. Chem. Soc.* **2002**, *124*, 2860–2861; c) R. A. Mehl, T. P. Begley, *Org. Lett.* **1999**, *1*, 1065–1066.
[6] a) A. Chandor, O. Berteau, T. Douki, D. Gasparutto, Y. Sanakis, S. Ollagnier-de-Choudens, M. Atta, M. Fontecave, *J. Biol. Chem.* **2006**, *281*, 26922–26931; b) A. Moysan, A. Viari, P. Vigny, L. Voituriez, J. Cadet, E. Moustacchi, E. Sage, *Biochemistry* **1991**, *30*, 7080–7088.
[7] a) G. Lin, L. Li, *Angew. Chem.* **2010**, *122*, 10122–10125; *Angew. Chem. Int. Ed.* **2010**, *49*, 9926–9929; b) J. Cadet, P. Vigny in *Bioor-*

ganic Photochemistry, Vol. 1, Photochemistry and the Nucleic Acids (Ed.: H. Morrison), Wiley, New York, **1990**.

[8] E. Bürckstümmer, T. Carell, *Chem. Commun.* **2008**, 4037–4039.

[9] a) M. G. Friedel, J. C. Pieck, J. Klages, C. Dauth, H. Kessler, T. Carell, *Chem. Eur. J.* **2006**, *12*, 6081–6094; b) M. G. Friedel, O. Berteau, J. C. Pieck, M. Atta, S. Ollagnier-de-Choudens, M. Fontecave, T. Carell, *Chem. Commun.* **2006**, 445–447.

[10] a) S. C. Silver, T. Chandra, E. Zilinskas, S. Ghose, W. E. Broderick, J. B. Broderick, *J. Biol. Inorg. Chem.* **2010**, *15*, 943–955; b) T. Chandra, S. C. Silver, E. Zilinskas, E. M. Shepard, W. E. Broderick, J. B. Broderick, *J. Am. Chem. Soc.* **2009**, *131*, 2420–2421; c) C. Mantel, A. Chandor, D. Gasparutto, T. Douki, M. Atta, M. Fontecave, P. A. Bayle, J. M. Mouesca, M. Bardet, *J. Am. Chem. Soc.* **2008**, *130*, 16978–16984.

[11] S. J. Kim, C. Lester, T. P. Begley, *J. Org. Chem.* **1995**, *60*, 6256–6257.

[12] M. Munzel, L. Lercher, M. Müller, T. Carell, *Nucl. Acids Res.* **2010**, *38*, e192.

[13] S. J. Johnson, L. S. Beese, *Cell* **2004**, *116*, 803–816.

[14] C. Biertümpfel, Y. Zhao, Y. Kondo, S. Ramon-Maiques, M. Gregory, J. Y. Lee, C. Masutani, A. R. Lehmann, F. Hanaoka, W. Yang, *Nature* **2010**, *465*, 1044–1048.

[15] a) A. F. Glas, E. Kaya, S. Schneider, K. Heil, D. Fazio, M. J. Maul, T. Carell, *J. Am. Chem. Soc.* **2010**, *132*, 3254–3255; b) M. J. Maul, T. R. Barends, A. F. Glas, M. J. Cryle, T. Domratcheva, S. Schneider, I. Schlichting, T. Carell, *Angew. Chem. Int. Ed.* **2008**, *47*, 10076–10080.

[16] J. C. Pieck, U. Hennecke, A. J. Pierik, M. G. Friedel, T. Carell, *J. Biol. Chem.* **2006**, *281*, 36317–36326.

[17] W. Kabsch, *J. Appl. Crystallogr.* **1993**, *26*, 795–800.

[18] Collaborative Computational Project Number 4, *Acta Crystallogr. Sect. D* **1994**, *50*, 760–763.

[19] A. J. McCoy, R. W. Grosse-Kunstleve, L. C. Storoni, R. J. Read, *Acta Crystallogr. Sect. D* **2005**, *61*, 458–464.

[20] P. Emsley, B. Lohkamp, W. G. Scott, K. Cowtan, *Acta Crystallogr. Sect. D* **2010**, *66*, 486–501.

[21] P. D. Adams, R. W. Grosse-Kunstleve, L. W. Hung, T. R. Ioerger, A. J. McCoy, N. W. Moriarty, R. J. Read, J. C. Sacchettini, N. K. Sauter, T. C. Terwilliger, *Acta Crystallogr. Sect. D* **2002**, *58*, 1948–1954.

[22] G. N. Murshudov, A. A. Vagin, E. J. Dodson, *Acta Crystallogr. Sect. D* **1997**, *53*, 240–255.

[23] See also, G. Lin, C.-H. Chen, M. Pink J. Pu, L. Li, *Chem. Eur. J.* **2011**, *17*, 9658–9668.

Received: January 18, 2011
Revised: May 5, 2011
Published online: July 20, 2011

